



UPPSALA
UNIVERSITET

Everything you wanted to know about the TPA molecule adsorbed on Au(111)

Author:

Pamela H.W. Svensson

Supervisor:

Barbara Brena

August 21, 2020

Abstract

The electronic properties of Triphenylamine (TPA) in gas phase and adsorbed on gold(111) have been simulated with Quantum Espresso using Density Functional Theory (DFT). To better understand how the presence of a gold surface affects sunlight absorption in the system, partial Density Of States (pDOS) and Near Edge X-ray Absorption Fine Structure (NEXAFS) of the system have been calculated. To describe the electronic excitation, three different methods have been used, No Core Hole (NCH), Full Core Hole (FCH) and Half Core Hole (HCH) approximation. The excitation of the TPA molecule was made in the nitrogen (N) atom and in the four different carbon (C) atoms with different electronic environments, C-ipso, C-ortho, C-meta and C-para. When using the HCH method, the absorbing atom must be described by a pseudopotential (PP) which includes half of a hole in the 1s orbital. This PP has been generated and a detailed summary of the process is described. The TPA/gold system relaxes to a position with the central N atom of TPA above an gold (Au) atom in the second layer of the surface and at a distance of 3.66 Å to the first layer. TPA keeps its symmetry with only small differences in the length of atomic bonds when adsorbed. The most striking result of this study is how the band gap of TPA is affected by the gold layer. From the pDOS we can observe that TPA in gas phase has a clear band gap of 2.2 eV with C-ortho dominating in the valence region and the four carbons dominating in the first unoccupied states. When depositing the molecule on the surface of Au(111), the band gap is essentially gone and a number of states appear between the previous highest occupied and lowest unoccupied molecular orbital in TPA. These new states align in energy with three clusters of states of the gold suggesting an interaction between the molecule and the surface. In the generated NEXAFS of nitrogen and carbon in TPA gas phase, one can observe a small pre-peak before the first unoccupied state. This is reinforced when adsorbing the molecule, which generates a pre-peak of approximately 3 eV in width. The pre-peak is connected to the new peaks seen in pDOS, correlating with experimental results on the same system.

Contents

1	Populärvetenskaplig Sammanfattning	3
2	Introduction	4
2.1	Organic and Perovskite Photovoltaics	4
2.1.1	Manufacturing and Applications	5
2.2	The molecular system and Spectroscopy	6
3	Overview of Density Functional Theory	7
3.1	Functionals and Basis Sets	9
4	Theoretical Spectroscopy	9
4.1	Photoelectron spectroscopy of the Core level	9
4.2	Spectroscopy of unoccupied levels	10
4.3	Pseudopotentials and how they can be generated	13
5	Density of States	15
6	Results	16
6.1	Geometry Optimization	16
7	Final Remarks	26
7.1	Conclusions and Outlook	26
A	Density of states with HCH approximation	27

1 Populärvetenskaplig Sammanfattning

Utvecklingen av solceller har öppnat för nya sätt att framställa grön energi. Varje år dyker det upp nya, innovativa material vilka kan ta tillvara på energin i solens strålar och göra om dessa till kemisk energi i solcellen, vilket i sin tur kan utvinnas och användas av elektriska apparater. Detta sker tack vare att elektronerna i solcellsmaterialet absorberar fotonerna från solljuset och använder denna energi till att hoppa till ett högre energitillstånd. Om det absorberade solljuset och antalet exciterade elektroner maximeras så kan materialet ge en högeffektiv solcell.

I denna rapport har modelleringen av materialet gjorts med täthetsfunktional-teori i datorsimuleringar med en molekyl kallad Triphenylamin (TPA) placerats på en guldtyta. TPA har tidigare används som en komponent i diverse solceller och guld är ett vanligt förekommande ämne i elektroder, interaktionen mellan TPA och guld är därför av intresse. Om energinivåerna i kropparna kan modelleras, så vet vi även hur elektronerna kan hoppa vid ljusabsorption och därmed hur materialet skulle kunna fungera i en framtida solcell.

TPA-molekylen och guldtytan simulerades inledningsvis i sitt grundtillstånd, det vill säga, när alla elektroner ligger så långt ner i energi som möjligt. Detta kan observeras i Figur 11 där energitillstånden för kolatomerna, kväveatomen osv. kan utläsas som toppar och dalar beroende på om det finns många eller få tillgängliga nivåer för elektronerna att befinna sig på. TPA-molekylen i gasform visas i Figur 11a med den sammanlagda mängden energitillstånd för de olika atomerna som linjen i svart. Mängden tillstånd ligger på 0 mellan den högsta ockuperade energinivån vid 0 eV (Fermienergin) och 2.2 eV (lägsta oockuperade energinivån). Det betyder att en foton med energi på minst 2.2 eV skulle kunna excitera en elektron i TPA. När molekylen däremot ligger på guldtytan så visar det sig att det dyker upp en mängd med tillstånd i området 0-2.2 eV, se Figur 11b. Detta betyder att elektronerna kan flöda fritt mellan olika energier och stör processerna som behövs inom en solcell.

Fortsättningsvis simulerades NEXAFS (Near Edge X-ray Absorption Fine Structure) vilket ger information om de oockuperade tillstånden i materialet. I experiment så belyses materialet så att elektronerna exciteras till högre energitillstånd för att sedan falla tillbaka igen. Detta ger upphov till nya fotoner strålar från materialet med energier motsvarande energin som skiljer mellan det högsta ockuperade tillståndet och de oockuperade tillstånden. Simuleringarna av NEXAFS i det här arbetet visar att nya oockuperade tillstånd dyker upp när TPA-molekylen känner av guldtytan, vilket överensstämmer med experiment gjorda på samma system. NEXAFS-resultaten styrker teorin från första delen i projektet, det vill säga, att elektronerna kan flöda fritt från högre till lägre energier. Denna insikt kan gynna framtida materialmodellering av material för solceller och ger upphov till nya frågor om hur andra ytor kan tänkas interagera med TPA-molekylen.

2 Introduction

The IPCC report of 2014 highlighted the dangers of what can happen if we let the mean temperature of earth rise three degrees and above [1]. Some obvious consequences are an increase of extreme weather, disappearing glaciers and devastating, harsh environments where animal- and plant life will struggle to survive. The higher mean temperature of the earth has its origin in the greenhouse effect, which traps solar radiation, allowing for a higher absorption of energy. The greenhouse effect is a natural part of the atmosphere, but as a result of over 200 years of excessive human produced fossil combustion, the CO₂ levels are at many 1000% higher than at the pre-industrial era. Governments and companies worldwide are therefore investing in carbon-neutral (or even carbon-positive) alternatives to supply us with the energy we need to continue and thrive in our communities. Solar cells are one part of this story, and this thesis focuses on a specific component, a material whose properties are essential for efficient harvesting of solar energy. The material in question is Triphenylamine (TPA) which has, thanks to its versatile properties, been of interest in several studies [2]. It has been shown to act as an important contributor to the development of organic light-emitting diodes and photovoltaics such as Organic Solar Cells (OSC) and Dye Sensitized Solar Cells (DSSC). These two novel types of Photo Voltaic Cells (PVC) may in the near future be able to challenge the widely used commercial silicon based solar cells. The intermolecular reactions which occur in a photoelectronic device, such as light absorption and charge transfer, are often localized in interfaces between molecules or molecule-surface. In this project, the electronic structure of Triphenylamine (TPA) has been studied, in gas phase as well as adsorbed onto the surface of gold (Au)(111). Density Functional Theory (DFT) via the Quantum Espresso package [3, 4] has been used to theoretically try to explain how the electronic states of the TPA behave upon adsorption. By using previous experimental results done on the same system, obtained at the ALOISA beamline by the group of Assoc. Prof. C. Puglia (Uppsala University), the methods to theoretically describe the atoms and excitations can be verified.

2.1 Organic and Perovskite Photovoltaics

Humanity has since pre-historic times strived toward the development of new tools and methods to make everyday life easier. From the first simple knives by the stone-age man, until automation in industries and smart homes. The industrial revolution, which has its beginning in the 18th century, was first aimed at the textile industry. Large, mechanised cotton spinning engines could suddenly increase the output with a factor of 500, in comparison with the average worker [5]. These machines were often driven by burning coal, and two centuries later, coal is still one

of the three big energy providers in the world (27%) alongside with oil (34%) and natural gas (24%). [1] In this project, focus will be on a very different energy source. As mentioned in the introduction, solar cells move the technology one step closer to a carbon free economy, and by that, decreasing the negative effect humanity has on our planet. Instead of harvesting the chemical energy stored in coal, solar cells make use of the high energy radiation emitted by the sun. By carefully designing the material in such a way so that the absorption spectra of the material matches the solar spectra to a great extent, a high efficiency solar cell can be created. An electron positioned in the Highest Occupied Molecular Orbital (HOMO) may absorb energy from the incoming solar photon, exciting it to an unoccupied state at a higher energy. High efficiency in the excitation process can be reached by exciting the electrons to the Lowest Unoccupied Molecular Orbital (LUMO), as an additional amount of absorbed energy will result in lost energy in the form of heat. To avoid recombination with the positively charged hole left behind in HOMO, a junction between an electron donor material and an electron acceptor material is often used in Organic Solar Cells (OSC). In Perovskite Solar Cells, a specific crystalline structure called Perovskite is used for light harvesting. The recombination is avoided by introducing an Electron-Transporting Material (ETM) with a LUMO slightly lower in energy, and a third material, known as the Hole-Transporting Material (HTM). By increasing the distance between the electron and the hole with ETMs, HTMs or donor/acceptor junctions, the attraction of recombination can be decreased, maintaining a high number of excited electrons in the system. The electrons and holes can thereafter be lead through an electrode creating a current which can be put to use.

2.1.1 Manufacturing and Applications

OSCs are often based on polymers but small molecules such as phthalocyanines and fullerenes are also a part of this particular research field [6]. The material can be manufactured by printing or coating from a solution in a continuous process, making it possible to manufacture a large volume at a small cost. This challenges the conventional fuels as a cost-effective renewable energy source. In addition, because of the flexibility of the material and low mass weight, OSCs has the opportunity to change the way we generate electricity in the society. From rigid and heavy solar panels on roofs or in big solar parks, to OSCs which can be integrated in new sectors, such as wearable technology or incorporated in the walls or windows in smart homes. In recent years, OSCs has finally started to make the first steps outside research facilities and into tech companies as a salable product. Some examples are Exeger Operations AB which has developed light-powered headphones, and Solarmer Energy Inc. which is developing and selling printed organic photovoltaic material, targeted at wearable technology.[7, 8]

2.2 The molecular system and Spectroscopy

Surface science techniques bring new insights in how atomic systems behave. By exciting the organic molecule with radiation of various wavelength one can get information about the intermolecular environment in chemical processes such as atomic and molecular bonding. This technique is known as spectroscopy and will be discussed more in detail in Section 4.

The molecule of interest in this study, TPA or N,N-diphenylaniline, $(C_6H_5)_3N$, was first synthesized by the chemists Merz and Weith in 1873 [9]. TPA has a nitrogen atom at its centre which is surrounded by three phenyl rings each having a co-planar carbon atom bonded to the nitrogen via sp^2 -hybridization. The three rings are twisted and give the molecule a propeller-like shape. This structure makes the formation of amorphous films possible, which can be used within optoelectronic devices and HTMs. In this project, calculations have been done with the molecule adsorbed on a sheet of Au(111), a common conductor used in electrodes, to try and get a better understanding of the chemical interface. Focus has been on studying the chemical environment of the N atom and the unequal C atoms C-ipso, C-ortho, C-meta and C-para, described in Figure 1, since these atoms in the TPA molecule are the most active in chemical reactions.

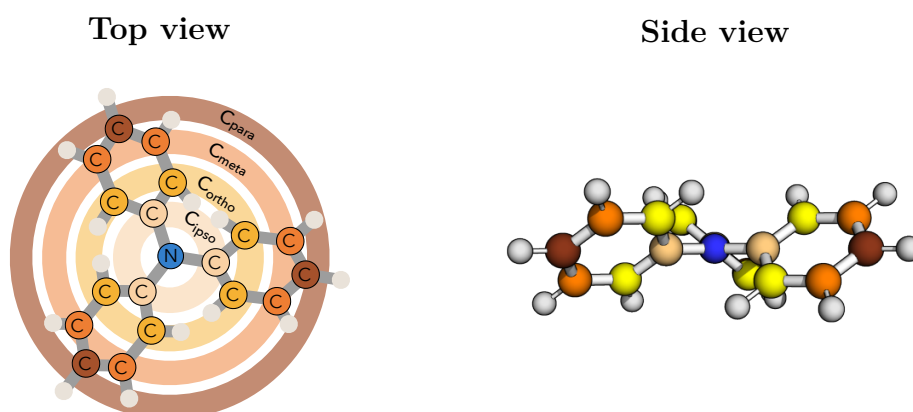


Figure 1: Molecular structure of TPA from above and side with four inequivalent carbon atoms, C-ipso, C-ortho, C-meta and C-para. The color scheme of the different species will follow through all figures in this thesis.

Previous research has stated the excellent electron donor and hole transport capabilities of TPA and it is therefore widely used in PVCs [2]. By using TPA as a base for dyes in DSSC, researchers have also received high photon to electron-conversion efficiencies [10, 11].

3 Overview of Density Functional Theory

Density functional theory (DFT) has become the preferred framework in theoretical material studies. In this section, DFT will be briefly introduced.

Consider a system of N nuclei and n electrons, all information is then contained in the many-body wavefunction, Ψ which satisfies the time-independent Schroedinger Equation

$$\hat{H}\Psi(\{R_I\}, \{r_i\}) = E\Psi(\{R_I\}, \{r_i\}) \quad (1)$$

with the Hamiltonian \hat{H} expressing all interactions within the system, $\{R_I\}$ the space coordinates of the nuclei and $\{r_i\}$ the space coordinates of the electrons, spin included. The Hamiltonian takes the following form

$$\hat{H} = \hat{T}_e + \hat{T}_N + \hat{V}_{ee} + \hat{V}_{NN} + \hat{V}_{Ne} \quad (2)$$

where the first two terms represent the kinetic energy operators of the electrons and nuclei, respectively, the third and fourth terms are the electron and nuclear Coulomb repulsion and the fifth term is the attraction between the nuclei and electrons. Expressing the Hamiltonian in the terms of the reduced Planck constant \hbar ($\hbar = h/2\pi$), the elemental charge e , the mass of the electron m_e , the mass of the nucleon M_I and the relative permittivity ε_0 we get,

$$\hat{H} = - \sum_{i=1}^n \frac{\hbar^2}{2m_e} \nabla_i^2 - \sum_{I=1}^N \frac{\hbar^2}{2M_I} \nabla_I^2 + \frac{1}{2} \sum_{i \neq j}^{n,n} \frac{1}{4\pi\varepsilon_0} \frac{e^2}{|r_i - r_j|} \quad (3)$$

$$+ \frac{1}{2} \sum_{I \neq J}^{N,N} \frac{1}{4\pi\varepsilon_0} \frac{Z_I Z_J e^2}{|R_I - R_J|} - \sum_{I,i}^{N,n} \frac{1}{4\pi\varepsilon_0} \frac{Z_I e^2}{|R_I - r_i|} \quad (4)$$

with the atomic number Z .

The task is now to find the molecular properties by calculating the molecular many-body wavefunction and thereby the eigenvalues. Approximations have to be made to achieve this. First and foremost, the Born-Oppenheimer Approximation, which decouples the Hamiltonian in an electronic and nuclear part. With electrons moving at a much higher speed than the nuclei, the nuclear kinetic part is neglected, and the nuclear repulsion term becomes a constant,

$$E_{NN} = \frac{1}{2} \sum_{I \neq J}^{N,N} \frac{1}{4\pi\varepsilon_0} \frac{Z_I Z_J e^2}{|R_I - R_J|} = C. \quad (5)$$

This reduces the electric Hamiltonian to a purely electronic problem and what is left is instead to solve the eigenvalue equation:

$$\hat{H}_e \Psi(\{r_i\}) = E_e \Psi(\{r_i\}) \quad (6)$$

where E_e is the total energy of the electrons. Considering only the nuclei, then the Hamiltonian can be written as

$$\hat{H}_n = - \sum_{I=1}^N \frac{\hbar^2}{2M_I} \nabla_I^2 + \mathcal{E}(\{R_I\}) \quad (7)$$

with $\mathcal{E}(\{R_I\})$ representing the potential energy surface in which one can find the lowest energy of the system, i.e. the optimized geometry. Thus the Hamiltonian can be separated in two parts, of which the electronic one is of primary interest for the calculations.

Returning to the electron-electron interaction term, then the wavefunction is still complicated. Since the effect of all the electrons is needed to be determined, Hohenberg and Kohn (H-K) proposed the idea of a one-to-one correspondence between wavefunction and the external potential \hat{V}_{ext} created by the nuclei [12]. The second theorem from H-K says that, in terms of the electron density $\rho(r)$, a universal functional $E(\rho)$ can be defined. The global minimum value of this functional in the potential \hat{V}_{ext} is the ground state of the system. Furthermore, the density ρ which minimizes the functional is then the ground state density $\rho_0(r)$.

We can now use the two H-K theorems and write the energy, as described by the electron density,

$$E(\rho) = T(\rho) + E_{ee}(\rho) + V_{ext}(\rho) \quad (8)$$

consisting the electronic kinetic energy $\hat{T}(\rho)$, the interaction term $\hat{E}_{ee}(\rho)$ and the external potential created by the nuclei $\hat{E}_{ext}(\rho)$.

From the H-K theorems discussed in the previous section, and the Kohn-Sham (K-S) ansatz [13] we can write the energy functional as,

$$E_{KS}(\rho(r)) = T_s(\rho) + E_{cl}(\rho) + E_{ext}(\rho) + E_{xc}(\rho) \quad (9)$$

with the kinetic energy of the non-interacting system $T_s(\rho)$, the classical part of the energy $E_{cl}(\rho)$, and the exchange and correlation functional $E_{xc}(\rho)$.

3.1 Functionals and Basis Sets

The exchange and correlation functional is the link between a system of interacting and non-interacting particles where the two most used ones are the Local Density Approximation (LDA) and the Generalized Gradient Approximation (GGA)[14]. LDA uses a simple approximation of a uniform electron gas (UEG) which can be expressed as

$$E_{xc}^{LDA}(\rho) = \int_r \varepsilon_{xc}^{UEG}(\rho) \cdot \rho dr \quad (10)$$

and works best for systems with a similar behaviour to a UEG, such as valence electrons in metals. In the system of a molecule on a surface, which this thesis is based on, the electron distribution is highly inhomogeneous and therefore the GGA functional is preferred.

GGA proposes that the density is slowly varying over the local space and the gradient of the local electron density, $\nabla\rho$, can be included. The exchange and correlation term can be written as,

$$E_{xc}^{GGA}(\rho) = \int_r \varepsilon(\rho, \nabla\rho) \cdot \rho dr \quad (11)$$

with

$$\varepsilon(\rho, \nabla\rho) = \varepsilon_x^{UEG}(\rho) \cdot F_{xc}(\rho, \nabla\rho) \quad (12)$$

including the exchange energy density of a UEG, $\varepsilon_x^{UEG}(\rho)$ and a dimensionless function $F_{xc}(\rho, \nabla\rho)$.

4 Theoretical Spectroscopy

4.1 Photoelectron spectroscopy of the Core level

Obtaining the Ionization Energy (IE) of the core electrons, the x-ray photoemission process can be used by means of X-Ray Photoelectron Spectroscopy (XPS). In this thesis, the focus lies on electrons from the C 1s and N 1s orbitals with regard to the TPA molecule. Chemical information can be obtained from these due to the sensitivity of the local electronic environment. Using K-S orbitals of a fictitious system, the IE is simply not the eigenvalues of the core levels. With the transition state method IE can theoretically be calculated as the difference between the system

in its ground state and in its ionic state with one electron removed from the 1s K-S orbital,

$$IE_{1s}^{KS} = E_{n-1}^{KS} - E_n^{KS}. \quad (13)$$

The IE can be determined using two Self Consistent Field (SCF) calculations where the electronic charge distribution reaches self-consistency with its own electrostatic field. The first calculation determines the total energy of the system in its ground state and the second calculation obtains total energy of the system with a hole in the 1s state. [15]

4.2 Spectroscopy of unoccupied levels

In order to obtain information complementary to XPS, Near Edge X-Ray Absorption Fine Structure (NEXAFS) spectroscopy can be used. NEXAFS gives information regarding the empty states of a sample through exposure of a set of X-rays of a certain wavelength. Rays with specific wavelengths excite core electrons leaving a positively charged hole behind, see Figure 2. The sudden change in the electronic environment of the atom will cause rearrangements of the energy levels and the hole will thereafter get filled by an electron from another level. The energy drop of the electron which fills the hole, will cause either an emission of a fluorescent photon or trigger the emission of an Auger electron through a coupling with the transition energy. If the excited electron comes from a 1s orbital then the absorption peak is classified as K-edge whereas if the origin is the 2s or 2p orbitals, the absorption peaks are named L-edges.

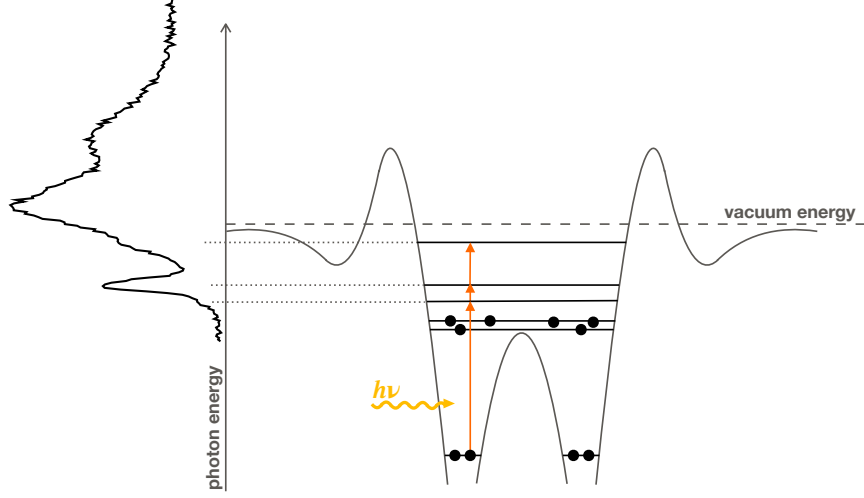


Figure 2: Schematic diagram of the physical process within the sample in a NEXAFS spectroscopy.

In this project focus has been on the C K-edge and, in particular, the N K-edge due to their role in the interaction between the TPA molecule and Au surface. In the transition of the electron from 1s orbital to its final state, the dipole approximation was used in order to get the transition probability

$$I \propto |\langle f | \hat{\chi} | 1s \rangle|^2. \quad (14)$$

with the dipole transition operator $\hat{\chi}$. The expectation value of the transition to the final state is proportional to the intensity I of the spectrum.

There are multiple ways of representing an excitation during a calculation. In a full core hole (FCH) approximation, one electron has been removed from the system, leaving a full hole in the core orbital and increasing the net charge by +1. A no core hole (NCH) approximation, on the other hand, keeps the system in its ground state. This method is useful when the core hole has minimal impact on the unoccupied states, such as in some metals. An excited core hole (XCH) approximation includes a full hole in the core and adds an additional electron in the valence band. The fourth method is the half core hole (HCH) approximation, which describes the superpositional nature of an electron being both in the core and in an excited state. This creates half a hole in the core orbital and adds half an electron in an excited state. In the main results of this work, HCH in the carbon 1s orbital and in the nitrogen 1s orbital was considered as such calculations has shown good agreement with the experimental spectral profiles [16, 15]. With the different excitation method, we can plot the spectrum of the TPA molecule in gas

phase. An example of how the FCH, NCH and HCH methods could look like and especially how different results these methods can provide in a N K-edge spectrum is shown in Figure 3.

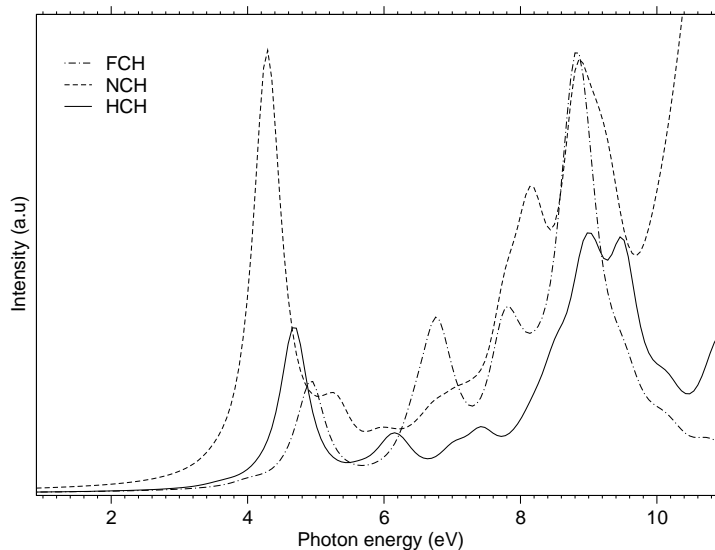


Figure 3: N K-edge spectrum using FCH, NCH and HCH method. The presence of half or a full core hole has a big impact on the shape of the calculated NEXAFS spectra and shows the importance of comparing the different approximations for each system of interest.

With the XSpecra code, a post processing tool in the QE package, one can simulate these core-hole effects with the help of PPs. The generation of a PP for different approximations is described in Section 4.3.

As illustrated in Figure 1, in TPA there are four C atoms in different chemical environment, resulting in four chemically non-equivalent C atoms. One has then to consider that the different chemical environments cause differences in the binding energy of the core 1s electrons, which are known as core level shifts (CLS). Depending on the entity of the shifts, these are observable in the photoelectron experiments as broadenings of the peaks, shoulders or multiple peaks. To obtain the proper BE for each different type of C we calculated the IE as described in Section 4.1. This calculation has to be repeated for each inequivalent atom and the relative CLS is then given by the respective energy difference.[16]

4.3 Pseudopotentials and how they can be generated

The complicated effects of core electrons are described in the Quantum ESPRESSO package as Plane-Wave basis set and Pseudopotentials (PPs) in the form of Projector-Augmented Waves (PAW) [17], Ultrasoft (US) [18] or Norm-Conserving (NC) [19]. These will replace the core electrons with a modified effective potential term and the valence electrons, which are active in chemical reactions, will be dealt with explicitly. Using the atomic code provided in QE one can generate a PP by using the following recipe.

To generate a PP one needs to construct an input file for the `ld1` code available in the atomic package. The first part includes the title, the atomic number `zed`, the type of functional `dft` and the electronic structure `config`.

```
input
  title='C',
  prefix='C',
  zed=6.0,
  config='1s1 2s2 2p1.5 3s0 3p0',
  iswitch=3,
  dft='PBE',
  rel=1
/
```

In the case of generating an ionized PP one can put a hole on the 1s state (1s1) or define fractional holes (1s1.5) and keep the atomic number the same.

The next section includes the name of the author and the PP filename which follows the naming convention: `atomic_symbol.description.UPF`. Here one can also choose if a NC, US or PAW PP is of interest by changing `pseudotype` and the angular momentum of the local channel. The `tm` keyword determines the pseudization model which in this case is set to the Rappe-Rabe-Kaxiras-Joannopoulos method. If spectroscopy calculations are of interest then the user has to include GIPAW information in the PP for the absorbing atom before running the QE spectroscopy tool, XSpectra. GIPAW information can mean many things, but the important part here is to include the presence of the all-electron wavefunction for the 1s core state. To include the GIPAW information the flag `lgipaw_reconstruction` is added and set to true. If a PP already has GIPAW information, this is then noted in the PP-filename with the ending `"_gipaw"`.

```
&inputp
  author='Pamela HW Svensson',
  file_pseudopw='C.star1s-pbemt_gipaw.UPF',
  pseudotype=2,
```

```
lloc=1,  
tm=.true.,  
lgipaw_reconstruction=.true.,  
upf_v1_format=.true.,  
/  

```

To extract the core wavefunction, which is needed to calculate NEXAFS, a tool provided in the XSpectra package called `upf2plotcore` can be used. At the time of writing, this code can only accept a PP file of version 1 and therefore include the tag `upf_v1_format` must be included. After the namelists `input` and `inputp`, the number of states is defined and the standard valence states configuration for generating a C PP is included.

```
2  
2S 1 0 2.0 0 1.5 1.5  
2P 2 1 1.5 0 1.5 1.5  
$test  
/  

```

To study a K-edge XAS transition, two P projectors for the 2P and 3P states must be included. One can also choose to include two S projectors for the 2S and 3S states.

```
4  
2S 1 0 2.0 0 1.5 1.5  
2P 2 1 1.5 0 1.5 1.5  
3S 2 0 0.0 0 1.5 1.5  
3P 3 1 0.0 0 1.5 1.5
```

The first column describes which projector is to be generated, the fourth is the occupation, the sixth and seventh columns describe pseudization radii.

After generating a FCH PP with the parameters presented, the user should now be ready to do a spectroscopy calculation.

1. Run a SCF calculation by using `pw.x` with a PP with NCH describing the absorbing atom, assuming the system is fully relaxed.
2. Thereafter, we can use the XSpectra code to find the fermi level of our system using the tag `calculation='fermi_level'`.
3. Extract the core wavefunction from the generated FCH PP with `upf2plotcore` and store it in the file format `".wfc"`.
3. When the input data for XSpectra is updated with the new fermi level `xe0`, and the location of the FCH core wavefunction is specified in the tag `filecore`, the calculation with XSpectra can begin. The

XSpectra code will then calculate the xanes cross section using the extracted core wavefunction from the generated FCH PP. If the goal is to do a HCH approximation, the SCF calculation is then run with a HCH PP in the absorbing atom, and the same PP is used to extract the core wavefunction for the XSpectra calculation.

4. Lastly, the CLS can be added to the generated spectra if the system contains atoms with unequal electronic environments.

5 Density of States

To better observe a change in the band gaps when applying the molecule on gold, Density of States (DOS) of TPA, both in gas phase and adsorbed on gold, has been calculated. DOS describes the number of states which can be occupied at each energy level. For a single junction solar cell, as an example, the theoretical optimum energy band gap is around 1.3 eV [20]. This can then easily be seen in a DOS plot of such a system with the HOMO peak and the LUMO peak around 1.3 eV apart in energy. A large peak indicates a large amount of available states at that energy level. If one would want to do a DOS calculation within the QE package, the user will have to follow these three steps assuming that the structure is fully relaxed.

1. Run a standard SCF calculation. If the DOS is done in the same directory as the geometry optimization calculation, this step can be skipped to save time.
2. Run a NSCF calculation with the flag `occupations='tetrahedra'` for a very accurate DOS. This will calculate the eigenvalues of the system starting from the previous SCF calculation.
3. Run the DOS calculation using the `dos.x` code provided in the QE package.

For a more detailed understanding of the generated DOS one can run an additional calculation with the code `projwfc.x` which produces a set of wavefunction files for each orbital in the system. These projected DOS (pDOS) can then be visualized in order to understand how the DOS of the system is built up.

6 Results

6.1 Geometry Optimization

To get reliable results when performing spectroscopy calculations on the system, an optimized structure where the energy is at its lowest has to be found. Three structures has been studied, where the N atom in the TPA molecule is above an Au atom of the first layer (TOP), of the second layer (HOL2) and of the third layer (HOL3).

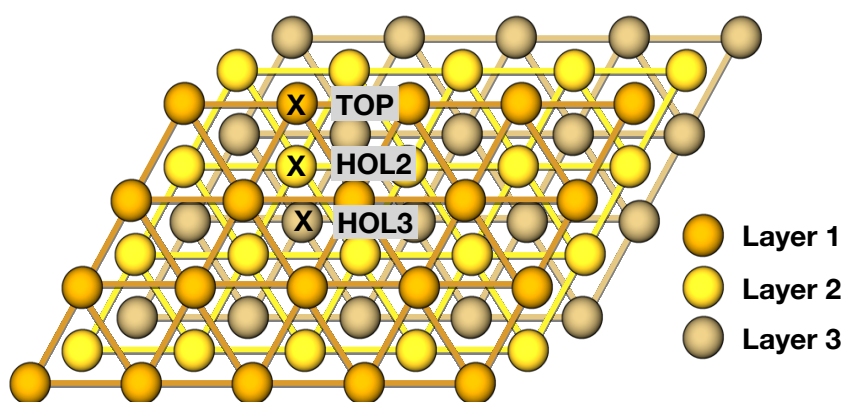


Figure 4: The three structures TOP, HOL2 and HOL3 of TPA on Au(111).

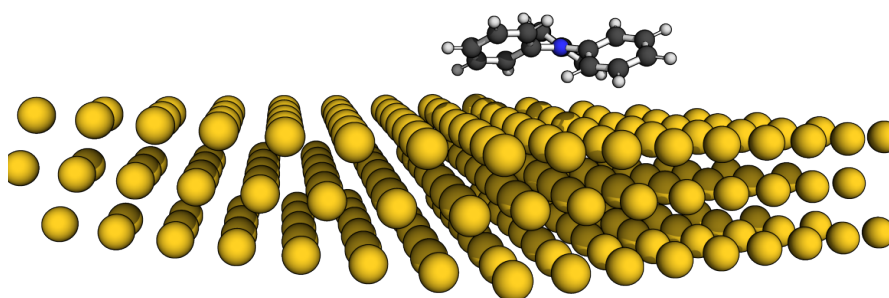


Figure 5: Supercell with TPA and three layers of gold atoms.

The monoclinic supercell was constructed with a basis of $23.53 \times 26.48 \text{ \AA}$ with 120° in between and a height of 25 \AA . The system included 216 Au atoms in three layers with the bottom two layers kept fixed and the TPA molecule was then added

a few Ångström above, see Figure 5. About 15 Å of vacuum is left between the adsorbed molecule and the next Au layer to avoid intermolecular effect. Ultrasoft PPs described the N, H and Au atoms and for the C atoms a Norm-Conserving PP was used. The system was then allowed to relax using BFGS quasi-newton algorithm at a cut-off energy of 90 Ry due to the Ultrasoft PPs being used. The total energy tolerance was kept at 10^{-3} (a.u) and the threshold of all components of all the forces was kept at 10^{-4} (a.u). A version of the GGA functional discussed in Section 3.1 called PBE [14], has been used for several configurations and to include the weak interactions between the molecule and the surface, van der Waal (vdW) interactions were modelled by the semi empirical variables of Grimme’s DFT-D3 [21].

After optimization of the three conformations TOP, HOL2 and HOL3, HOL2 was noted at the lowest energy. Therefore from now on, the results of TPA deposited on Au will be presented for HOL2. The system relaxed at a distance of 3.66 Å between the nitrogen atom and the first layer of gold. The C-ortho and C-meta atoms have a distance to the first gold layer of 2.97 Å and 2.96 Å, respectively. The bond between C-ortho and C-meta is therefore close to parallel with the first layer of gold, see Figure 6. The bond lengths in TPA in gas phase and adsorbed on gold can be seen in Table Figure 1.

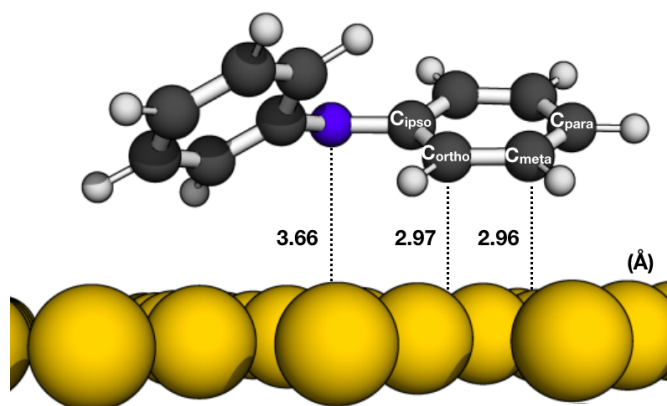


Figure 6: Distances from several atoms in TPA to first layer of gold. One of the phenyl rings in TPA has been removed for clarity.

The interatomic distances in TPA are around 1.40 Å and only small changes can be noted when adsorbed on Au(111). The lack of big changes in bond lengths indicates that the molecule is not distorted and remains in a symmetric shape after deposition. It could also mean that the interaction with the surface is weak.

	TPA gas	TPA/Au
N – C _{ipso}	1.42 Å	1.42 Å
C _{ipso} – C _{ortho}	1.40 Å	1.41 Å
C _{ortho} – C _{meta}	1.39 Å	1.39 Å
C _{meta} – C _{para}	1.40 Å	1.39 Å

Table 1: Intermolecular distances in TPA in gas phase and adsorbed on gold.

The N K-edge NEXAFS spectra in Figure 7 have been calculated with a gaussian smearing of 0.068 eV and with a HCH PP representing the nitrogen atom. At a first glimpse, one can note that the calculated NEXAFS spectra follows the curvature of the experimental data well, both in TPA gas phase and in HOL2 formation. The first N LUMO peak is dominated by states with a polarization in a direction normal to the surface (GI) until at 403 eV where polarization a direction parallel to the surface is more apparent. Since the molecule is adsorbed on the Au layer in the xy plane, it is possibly the P_z orbitals that account for the majority of the absorption normal to the atomic plane. One of the important questions motivating this study is to understand the origin of the experimental pre-peak when the TPA molecule is adsorbed on gold. The pre peak appears in the experimental setup in the range of 398.5-401.5 eV in Figure 7b. The calculated NEXAFS spectra has an occurrence of a pre-peak in the region of 399-400 eV. The theoretical pre-peak shows a dominance of states normal to the atomic plane, which is more apparent when we focus on this energy scale in Figure 8. Both the experiment and the calculations imply that something is happening when the TPA molecule is deposited on gold, and it is in the direction normal to the plane where the change occurs. Since NEXAFS spectra give information about unoccupied states, a pre peak could give indication about additional states appearing when the gold layer is present.

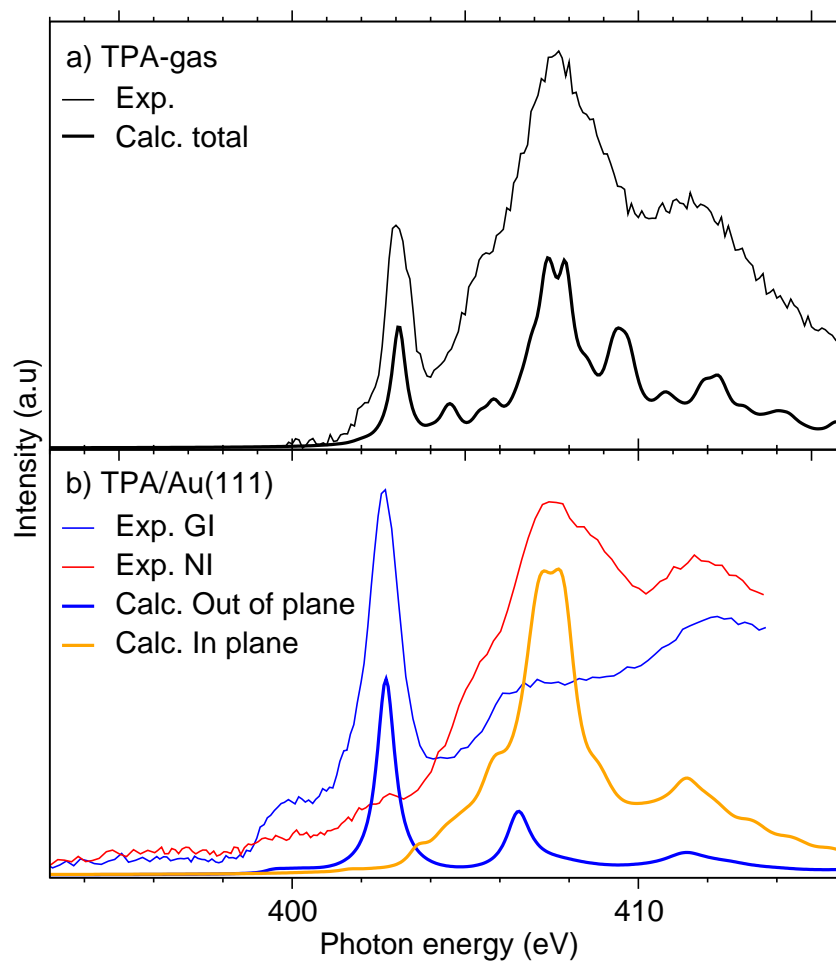


Figure 7: N K-edge calculation in comparison with experimental data. Polarization in the direction normal to the plane (GI) shows a clear contribution in the first peak at 402.8 eV.

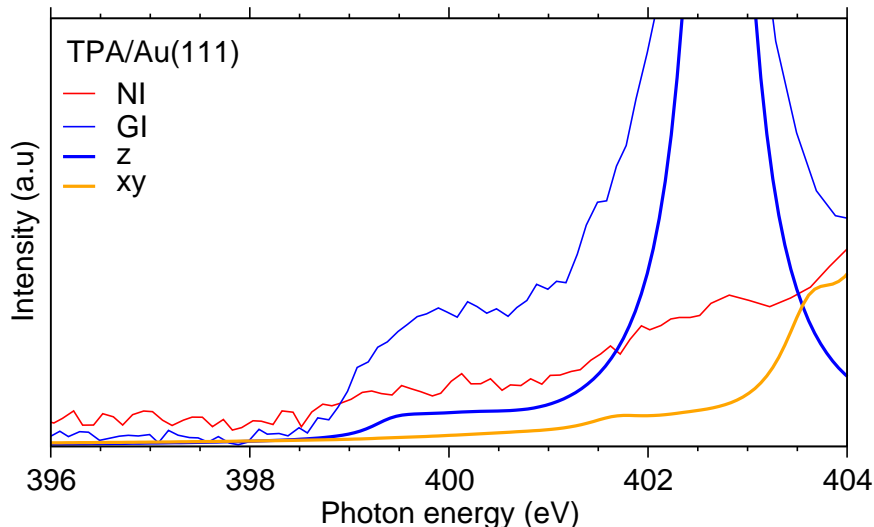


Figure 8: N K-edge spectrum with a focus on the energy range in which the pre peak occurs. The width of the pre peak is about 2-2.5 eV and is dominated by states in the direction normal to the plane. The calculated pre-peak clearly follows the energy range of the experimental data.

When calculating the C K-edge, a slightly different approach has to be made. As mentioned earlier, CLS has to be taken into account for the different C atoms in the TPA molecule. Table 2 shows the calculated CLS which has been added to the C K-edge spectra for TPA in gas phase and adsorbed on gold. The spectra are then mutually shifted to match the experiment.

	TPA gas	TPA/Au(111)
C _{ipso}	0.978 eV	1.041 eV
C _{ortho}	-0.330 eV	-0.425 eV
C _{meta}	-0.152 eV	-0.155 eV
C _{para}	-0.496 eV	-0.461 eV

Table 2: Table of core level shift for different C species in the TPA molecule. The shifts are added to the calculated C K-edge spectra resulting in Figure 9

Figure 9 shows the calculated NEXAFS spectra of the different carbon species in comparison with experimental results. TPA in gas phase and adsorbed on the gold surface results in spectra with a first peak predominantly consisting of C-ortho, C-meta and C-para. The second peak is in both cases mainly consisting of

C-ipso. This is expected since the electrons in C-ipso are affected by the presence of the nitrogen atom. Nitrogen has an electronegativity of 3.04 on the Pauling scale in comparison with 2.55 for carbon, and will therefore pull the electrons harder towards itself. In Figure 9, additional peaks can be seen at 282.5 eV for the calculated C-ortho and C-para atoms and at 284 eV for the C-ipso atoms. The extra peaks are not present in the experimental results for the same system nor in C K-edge spectrum of TPA/Au(111). The presence of the additional peaks are likely results of the generated HCH PP for carbon and are called ghost states. Such states can be created during the PP generation and more testing needs to be done to confirm the validity of the pseudopotential.

Similar to the N K-edge spectrum of TPA deposited on gold, a small pre peak can also be seen in the C K-edge spectrum in Figure 9b, both in experiment and in the theoretical results. One can note that the calculated NEXAFS of Figure 9b spectra indicates that something is happening at 2 eV before the big peak at 285 eV whereas in Figure 9a, that region appears to be empty. Since the Gaussian smearing in the calculations are set to 0.068 eV, this can be excluded of being the reason for a change happening almost 2 eV away from the first big peak. The second big peak in the C K-edge spectra of TPA/Au(111) is due to the shift in energy of the unoccupied states in the C-ipso atoms, mainly. One can also carefully mention that the third big peak in Figure 9b could be attributed to the second peaks of C-meta and C-para atoms. However, when moving higher in energy, the validity of the results becomes more uncertain.

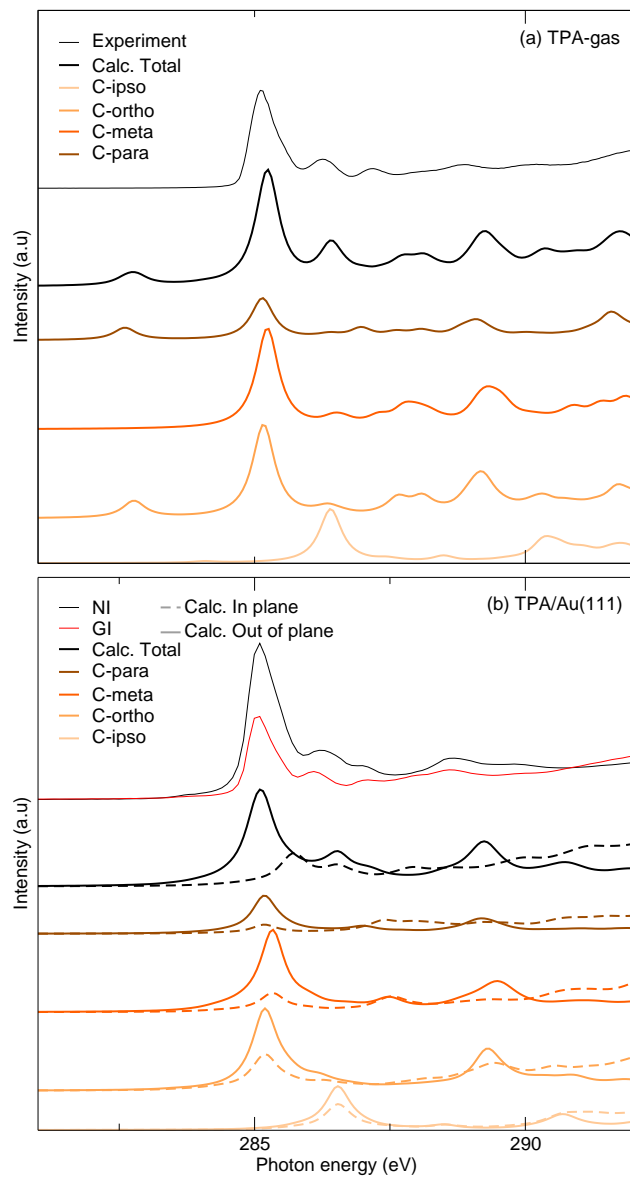


Figure 9: NEXAFS C K-edge of a) TPA in gas phase and b) TPA adsorbed on Au(111), both spectra are calculated within HCH approximation.

To get a full picture of the interaction between the molecule and the surface, one also need to take into account the occupied states and what is happening at the gap between HOMO and LUMO of the TPA molecule.

Using the techniques described in Part III.3 and IV, DOS and pDOS have been generated for the TPA in gas phase as well as adsorbed on Au(111). In Figure 10 a comparison can be seen of pDOS of TPA in gas phase in its ground state calculated in this study, with results taken from literature [9]. The nitrogen contribution has been enlarged for an easier comparison of the peak. The relative contributions to the valence region are similar in both spectra. HOMO is mainly dominated by C-ipso, C-ortho and C-para and only a small contribution could be observed from C-meta. The LUMO consists of all the C atoms and the first big peak of the unoccupied states in the nitrogen atom cannot be seen until at about 4 eV from the HOMO region. The overall shape of the calculated DOS using generated PPs aligns with results from literature [9]. The PPs are therefore considered capable of describing the electronic structure in TPA and a gold surface can be added. Calculated DOS using HCH PPs are attached in Appendix A.

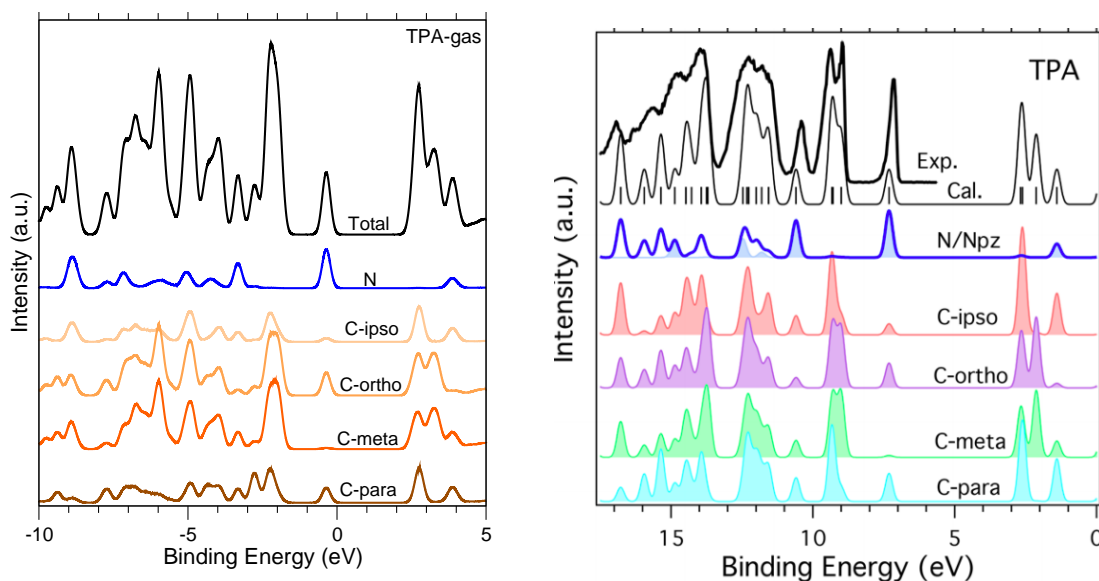


Figure 10: DOS and pDOS of TPA in gas phase calculated at the ground state (left) and a reference pDOS taken from literature (right)[9].

In Figure 11 one can observe the contributions of different species of carbon as well as nitrogen and gold at ground state. The pDOS contribution of the gold layer is reduced in size to 3 % of the original data for graphical purposes.

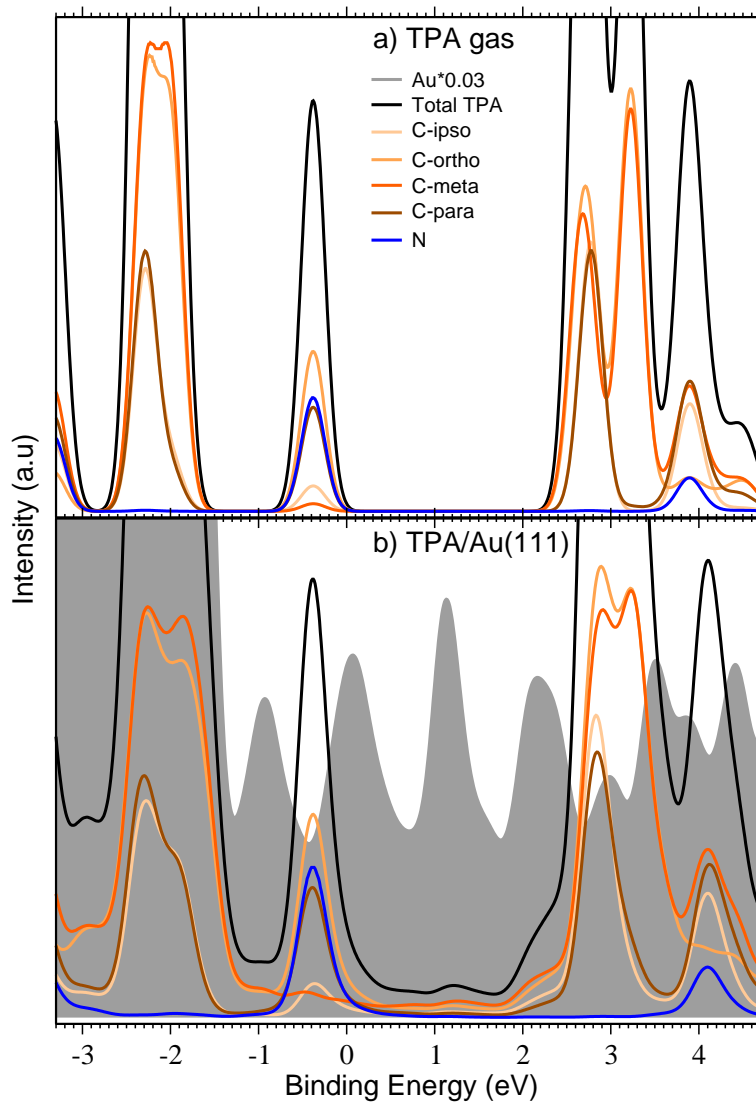


Figure 11: pDOS of a) the TPA molecule in gas and b) adsorbed on Au(111). A striking difference is the appearance of states in energies between the Fermi energy at 0 eV and at about 2.3 eV when the TPA molecule is adsorbed in comparison with the gaseous state.

In gaseous phase, the energy region of 0-2.3 eV is completely empty with a clear band gap but in the presence of the gold surface, multiple states can now be observed. In TPA, the biggest contributions to the new intermediate states are coming from the four species of carbon. The valence region of the molecule in both 11a and 11b are strongly affected by the C-ipso, C-para and the N atom whereas the LUMO region, i.e. around 2.3 eV, both cases are mainly dominated by the carbon atoms only. A strong contribution of nitrogen to the unoccupied states cannot be seen until around 4 eV in both cases. In Figure 11b, a correlation can be noted at 1.1, 2.1 and 3.0 eV where the peaks of Au coincides with peaks of the carbon and nitrogen atoms. This becomes even more apparent in Figure 12 suggesting an interaction between the nitrogen in TPA and the gold layer. The new states appearing in this region are at the beginning of the NEXAFS N K-edge spectrum in Figure 7b.

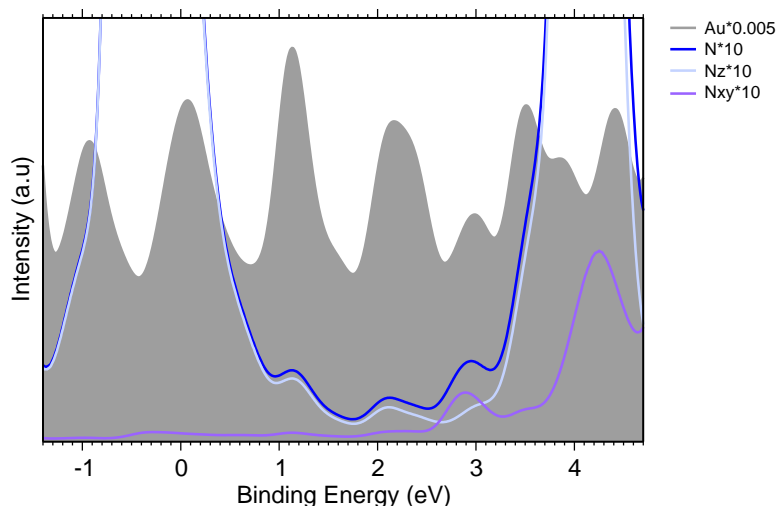


Figure 12: pDOS of TPA molecule adsorbed on Au(111). Intermediate states of nitrogen in the energy region 0-4 eV of the TPA molecule.

Figure 12 does also indicates, that the intermediate N states are covered by orbitals normal to the gold surface as well as parallel with the gold surface.

7 Final Remarks

The calculations in this study have been performed with PBE functional. PBE is however known to underestimate band gaps and the hybrid functional B3LYP could therefore be better suited for the spectral calculations [22]. B3LYP was not implemented in the XSpectra code during the period of this study, but if this would change in the future, additional calculations could bring new insights in the change of the HOMO-LUMO gap of TPA during adsorption. The usage of Grimme’s DFT-D3 for vdW contribution is motivated with it being a model which has shown to provide accurate adsorption distances in the past [23], furthermore, other types of vdW models should be investigated to see if they would bring a similar result. The calculations in this study have been to a large extent performed using generated HCH PPs to describe the absorbing atom in question. Since some results indicate the presence of virtual states, observed in C K-edge spectra of TPA in gas phase, the PPs must be handled with care and more testing is required before continuing with more elaborate studies. The small changes in NEXAFS for the two approximations made us also certain that the ghost states would not affect the result to a greater extent. This becomes clear when the ghost states are no longer visible when calculating NEXAFS with the gold layer present.

7.1 Conclusions and Outlook

Calculated spectra and DOS have given a unified result of new states appearing when the TPA molecule is adsorbed on gold. The relaxed TPA/Au structure prefers keeping the nitrogen atom above a gold atom in the second gold layer. The distance of 3.66 Å between nitrogen and the first gold layer suggests a physisorption, whereas the DOS and NEXAFS results indicate a strong interaction occurring between the two bodies, and thus giving rise to the pre peak observed in experiments. The generated pseudopotentials provided an acceptable description of the absorbing atoms, even though a few ghost states were visible in the C HCH PP. The additional states in the band gap that we have found indicate that the electronic structure of TPA is strongly affected by the adsorption on the Au(111) surface. Therefore, the molecules directly bonded to this gold surface do not have the same properties as those which are free, the main issue being the extreme narrowing of the HOMO-LUMO gap. This is an important conclusion due to the fact that gold is often used as a lead in solar cells and in other types of optoelectronic devices. It shows that the bonding of TPA is not fully understood, and its impact on the electronic structure of the molecule is much stronger than would be expected for a physisorption. With TPA being the base for many DSSC and other types of solar devices, it would be important to continue to study the interaction of TPA with different types of materials to understand how this can affect the functionality of solar cells.

A Density of states with HCH approximation

We had performed a calculation of the DOS of TPA on Au(111) with and without N1s core hole (i.e. in the HCH approximation and in the ground state respectively). The reason was to verify whether the extra electronic states between the HOMO and LUMO of TPA were present already in the ground state or if they appeared only after the excitation of the N1s. In the first case, which turned out to be true as discussed in the present thesis, the extra states are an initial state effect, due to new states formed by the adsorption of TPA on the Au(111) surface. If the states had only appeared in the DOS of the excited system and not in the DOS of the ground state, it would have implied that the extra peak in the N Kedge spectrum was a final state effect. The formation of the extra states would have been coupled to, and would have been caused by, the creation of the core hole. By finding out that it is an initial state effect, coupled to the bonding of TPA on the gold surface, our analysis gave an answer to a long debated issue.

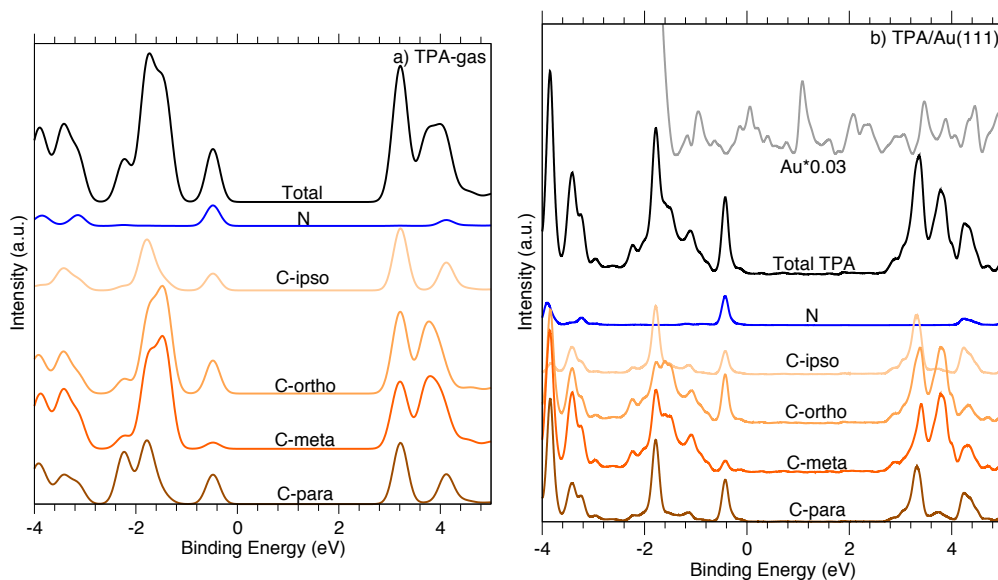


Figure 13: PDOS of TPA molecule a) in gas phase and b) adsorbed on Au(111) within HCH approximation. New states can be seen in the region 0-2.7 eV when the gold layer is present. Additionally, a pre peak to the unoccupied peak at 2.9.

Acknowledgments

I would like to take a few moments and thank everyone that helped and supported me during this masters project. Barbara, who guided me along the way, and Biplab, who was kind enough to be the subject reader. Big thanks to prof. Guido Fratesi who helped us understand the mysteries of CLS and also colleagues and friends from the server room and the Materials Theory division. My family that believes in my dreams. And finally, Max, who was being patient with a stressed out girlfriend and encouraged me to keep on going towards future PhD studies. Who knew that I also could do scientific stuff?

References

- [1] Rajendra K et. al Pachauri. *Climate change 2014: synthesis report. Contribution of Working Groups I, II and III to the fifth assessment report of the Intergovernmental Panel on Climate Change*. Ipcc, 2014.
- [2] SanYin Qu, JianLi Hua, and He Tian. New d- π -a dyes for efficient dye-sensitized solar cells. *Science China Chemistry*, 55(5):677–697, 2012.
- [3] Paolo et. al Giannozzi. Quantum espresso: a modular and open-source software project for quantum simulations of materials. *Journal of physics: Condensed matter*, 21(39):395502, 2009.
- [4] Paolo et. al Giannozzi. Advanced capabilities for materials modelling with quantum espresso. *Journal of Physics: Condensed Matter*, 29(46):465901, 2017.
- [5] Robert U Ayres. Industrial metabolism. *Technology and environment*, page 17, 1989.
- [6] Pamela Svensson. Dft investigations of the donor-acceptor couple cupc/c60, 2016.
- [7] Exeger Operations AB. Endless music experience true mobility with light-powered headphones. <https://exeger.com/applications>. Accessed: 2020-04-28.
- [8] Solarmer Energy Inc. Solarmer energy. <http://solarmer.com/aboutus>. Accessed: 2020-04-28.
- [9] Teng et. al Zhang. Lone-pair delocalization effects within electron donor molecules: the case of triphenylamine and its thiophene-analog. *The Journal of Physical Chemistry C*, 122(31):17706–17717, 2018.
- [10] Takayuki et. al Kitamura. Phenyl-conjugated oligoene sensitizers for tio2 solar cells. *Chemistry of Materials*, 16(9):1806–1812, 2004.
- [11] Marappan Velusamy, KR Justin Thomas, Jiann T Lin, Ying-Chan Hsu, and Kuo-Chuan Ho. Organic dyes incorporating low-band-gap chromophores for dye-sensitized solar cells. *Organic Letters*, 7(10):1899–1902, 2005.
- [12] Pierre Hohenberg and Walter Kohn. Inhomogeneous electron gas. *Physical review*, 136(3B):B864, 1964.

- [13] Walter Kohn and Lu Jeu Sham. Self-consistent equations including exchange and correlation effects. *Physical review*, 140(4A):A1133, 1965.
- [14] John P Perdew, Kieron Burke, and Matthias Ernzerhof. Generalized gradient approximation made simple. *Physical review letters*, 77(18):3865, 1996.
- [15] L Triguero, LGM Pettersson, and H Ågren. Calculations of near-edge x-ray-absorption spectra of gas-phase and chemisorbed molecules by means of density-functional and transition-potential theory. *Physical Review B*, 58(12):8097, 1998.
- [16] Guido Fratesi, Valeria Lanzilotto, Luca Floreano, and Gian Paolo Brivio. Azimuthal dichroism in near-edge x-ray absorption fine structure spectra of planar molecules. *The Journal of Physical Chemistry C*, 117(13):6632–6638, 2013.
- [17] Peter E Blöchl. Projector augmented-wave method. *Physical review B*, 50(24):17953, 1994.
- [18] David Vanderbilt. Soft self-consistent pseudopotentials in a generalized eigenvalue formalism. *Physical review B*, 41(11):7892, 1990.
- [19] DR Hamann. Optimized norm-conserving vanderbilt pseudopotentials. *Physical Review B*, 88(8):085117, 2013.
- [20] Sven Rühle. Tabulated values of the shockley–queisser limit for single junction solar cells. *Solar Energy*, 130:139–147, 2016.
- [21] Stefan Grimme. Semiempirical gga-type density functional constructed with a long-range dispersion correction. *Journal of computational chemistry*, 27(15):1787–1799, 2006.
- [22] Ks Kim and KD Jordan. Comparison of density functional and mp2 calculations on the water monomer and dimer. *The Journal of Physical Chemistry*, 98(40):10089–10094, 1994.
- [23] Alexander et. al Schlimm. Influence of a metal substrate on small-molecule activation mediated by a surface-adsorbed complex. *Chemistry–A European Journal*, 24(42):10732–10744, 2018.